

MODELLING OF THE WAX INJECTION PROCESS FOR THE INVESTMENT CASTING PROCESS: PREDICTION OF DEFECTS

Jean-Christophe GEBELIN, Aleksander M. CENDROWICZ and Mark R. JOLLY

IRC in Materials Processing, The university of Birmingham, Edgbaston, Birmingham B15 2TT, UK

ABSTRACT

Wax injection is the first step of the investment casting process. It is therefore an essential step, as many of the defects created in the wax can be reproduced in the final casting if they are not detected. This paper will present the models set up and experimentation carried out to validate these models. The numerical simulation has been carried out using MoldFlow[®] and Flow-3D[®]. MoldFlow[®] is a simulation package developed for the plastics industry whereas Flow-3D[®] is a more general CFD package. The models available in each of the packages are therefore different. For example, the wax exhibits non-Newtonian behaviour and can be modelled with a second order model, used in MoldFlow[®], or with a Carreau model, as in Flow-3D[®]. The density has also been described as function of temperature and pressure using two different phenomenological models. The emphasis in this paper will be made on the prediction of the appearance of two kinds of defects, weld lines that are surface defects, and air entrapment in the wax that can create residual stresses and distortion of the wax pattern produced. Some conclusions on the capability of the models and of the different simulation packages used will be drawn.

NOMENCLATURE

- μ dynamic viscosity
- μ_∞ infinite viscosity, i.e. viscosity for infinite shear rate
- μ_0 zero viscosity, i.e. viscosity for null shear rate
- λ phase shift, i.e. the inverse of the shear rate for which the viscosity start to change from μ_0 to μ_∞ in increasing shear rates
- n sensitivity of the viscosity to the shear rate during the transition from μ_0 to μ_∞ or vice-versa
- T temperature
- p absolute pressure
- ρ density
- T_0 gel temperature of the wax
- ρ_0 density at temperature T_0 and pressure $p=1$
- k_p compressibility factor
- k_t thermal expansion factor
- β coefficient of the density model without real physical meaning
- ψ coefficient of the density model without real physical meaning

INTRODUCTION

The Investment Casting process consists of making a replica of the desired part in an 'easy to form' material, and then to build-up a mould around that replica. Nowadays, in the casting industry, this mould is called the shell, and is made of layers of ceramic material. The

modern process used in the industry requires the removal of the replica from the mould, before casting, in order to avoid pollution of the cast metal with residues from the combustion of the replica. That is one reason for the use of wax to make the replica that can then be 'easily' removed by heating the mould. The waxes used are complex blended materials that usually contain natural waxes, resins and fillers in order to tune their mechanical and thermal properties. They may be injected in a liquid or paste state, depending on the application and geometry. It appears that the wax injection process can be carried out with materials presenting a wide range of properties, depending on the composition used and the state of the wax during the injection. Therefore an accurate investigation of the thermo-physical properties of the wax is necessary if modelling of the process is to be considered. Industrial waxes have not been widely studied although it is possible to find some data, Chakravorty (1999), that show how different the properties can be from one wax to another. Another study, Sigfried *et al* (2000), shows how the behaviour of the wax can be dependant on composition (i.e. resin content). From these studies, it appears that all the thermo-physical data needed to model the wax injection process should be measured before starting any simulation work.

The work presented here is dedicated to wax injection. Wax injection is being studied and modelled by considering one commercial wax. The wax used was a filled wax made of a blend of waxes (mainly paraffin and micro-crystalline), about 30% resin and about 40% of cross linked polystyrene.

Numerous experiments have been carried out in order to characterise the wax. Flow visualization experiments have also been performed, in order to validate the models that have been developed. This validation has been done by comparing simulation and experimental results of die filling, using different dies and two different simulation packages. Some conclusions are drawn.

MODEL DESCRIPTION

The wax exhibits a non-Newtonian behaviour that can be modelled with different models. In our work, as we have used two different simulation packages using each their own models, two different models have been identified. In Flow-3D[®], a Carreau model is used, whereas in MoldFlow[®] it is a second order model. The Carreau model used in Flow-3D[®] has been customized by developing user subroutines in order to have a more sophisticated temperature dependency of the viscosity.

Rheology

In order to be able to identify the rheological behaviour of the wax during the injection, its viscosity has been measured in a range of shear rates and temperatures. This work has been carried out on an industrial investment casting wax, Hyfill B417DER. The experimental investigation of the viscosity has been performed using two different techniques, capillary rheometry for the lowest temperature (paste and nearly solid state) and cone and plate rheometry for the highest temperatures (paste and liquid state). Both techniques have practical limitations that didn't allow the identification of the rheology over the full range of temperature with a single technique. A good agreement between the techniques has been observed in the overlapping range of temperature.

Carreau's model

Carreau's model describes the evolution of the viscosity versus temperature and shear rate through equation 1.

$$\mu = \mu_{\infty} + (\mu_0 - \mu_{\infty}) \left[1 + (\lambda \dot{\gamma})^2 \right]^{\frac{n-1}{2}} \quad (1)$$

From the viscometry experiments, the value of the different parameters, μ_{∞} , μ_0 , λ and n are determined at each temperature, and then a function is determined for each of the parameters to fit its evolution with temperature. A user sub-routine has been written for Flow-3D[®] in order to be able to use complex functions to describe the evolution of the parameters with temperature.

Second order model

The second order model used in MoldFlow[®] is described by equation 2

$$\ln \mu = A_1 + A_2 \ln(\dot{\gamma}) + A_3 T + A_4 (\ln(\dot{\gamma}))^2 + A_5 \ln(\dot{\gamma}) T + A_6 T^2 \quad (2)$$

Experimental viscometry data are entered in MoldFlow[®], and the model is fitted and the values of A_1 , A_2 , A_3 , A_4 and A_5 are determined.

Thermal properties

Thermal properties have been measured for the wax used. The heat capacity has been measured by Differential Scanning Calorimetry, the heat conductivity has been measured by C-MOLD Polymer Laboratories¹. The transitions temperatures, from liquid to paste and from paste to "solid" have been determined from the DSC experiments as well.

Heat conductivity

The heat conductivity is assumed constant in MoldFlow[®], and Flow-3D[®]. Therefore a single value has been used in both cases.

Heat capacity

The heat capacity measured from the DSC has been entered as function of temperature in a tabular way in Flow-3D[®] and a single value has been used in MoldFlow[®]. In the latest version of MoldFlow[®], the heat capacity can as well be entered as function of temperature, in a tabular way.

Density

The density has been measured by C-MOLD Polymer Laboratories as a function of pressure and temperature (PVT). From these experiments, the density has been input in Flow-3D[®] using a user sub-routine to calculate the density from equation 3

$$\rho = \rho_0 + k_p \log_{10}(p) - k_t (T - T_0) - \beta \tanh\left(\frac{T - T_0}{\psi}\right) \quad (3)$$

In MoldFlow[®], a two-domain tait model is used to describe the evolution of the specific volume ($1/\rho$) as function of the pressure and temperature. The specific volume is then calculated from equation 4

$$\frac{1}{\rho} = V_0(T) \left[1 - 0.0894 \ln\left(1 + \frac{P}{B(T)}\right) \right] \quad (4)$$

$V_0(T)$ is given by equation 5

$$V_0(T) = b_1 + b_2 (T - b_5) \quad (5)$$

and $B(T)$ by equation 6

$$B(T) = b_3 \exp[-b_4 (T - b_5)] \quad (6)$$

This is called a two-domain model as it defines two different domains, above and below a transition temperature T_{trans} . This transition temperature is defined by equation 7

$$T_{trans} = b_5 + b_6 P \quad (7)$$

There are two sets of values for b_1 , b_2 , b_3 and b_4 , one for a temperature lower than the transition temperature and one for a higher temperature.

FLOW PREDICTION

To validate the prediction of the models, different sets of experiments have been carried out. For the prediction of the filling, in the liquid state, a die has been designed to replicate the problem of going from thin to thick section. Fig.1 presents the different ingate configurations that this die allows, on the left, the first ingate position, in the middle of the bottom face, in the middle the second position in the bottom of the lateral face, and on the right the third position in the centre of the lateral face. For the prediction of the filling in the paste state, a die designed to study critical velocities in the ingate has been used. Fig.2 presents a schematic of the experimental apparatus. In these experiments, both liquid and paste injection has been used, so the simulation of these experiments has allowed us to validate our model in the paste condition.

Thick-thin die

These simulations have been carried out using Flow-3D[®]. The aim of these numerical simulations was to examine the predictive capability of the model with different ingate positions.

Different injection machines have different ways of controlling the flow of the wax during filling. Some machines can be controlled by applied pressure, some by flow rate. In both cases, the pressure applied is most of the time displayed on the machine, or even recorded for quality or other purposes. The main problem is that the pressure measured by the machine is never the pressure at the entrance of the die, but in the best cases the pressure in the nozzle. To carry out a reasonable simulation, reasonable boundary conditions are needed. As the geometry of the nozzle is not usually modeled, the

¹ C-Mold, 2353 North Triphammer Road, Ithaca, New York 14850, USA

pressure at the boundary, which will be in this case the entrance of the die, needs to be known. Therefore, the pressure in the entrance of the die was recorded during the experiments with a pressure transducer and has been used as a boundary condition. Fig.3 shows the pressure recorded at the entrance of the die in the case of the lateral ingate situated in the middle of the face (position shown on the left of Fig. 1), with a nominal pressure of 2.5 MPa (25 bars).

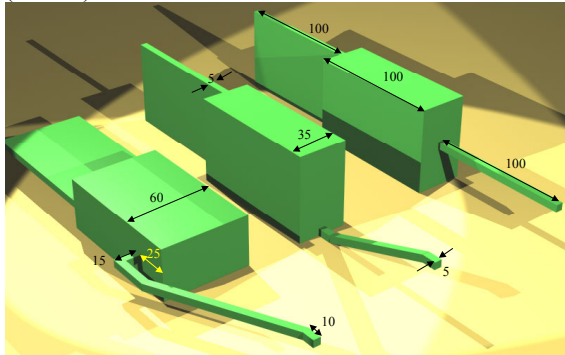


Figure 1: Schematic showing the 3 different possible ingates in the thick-thin die experiment.

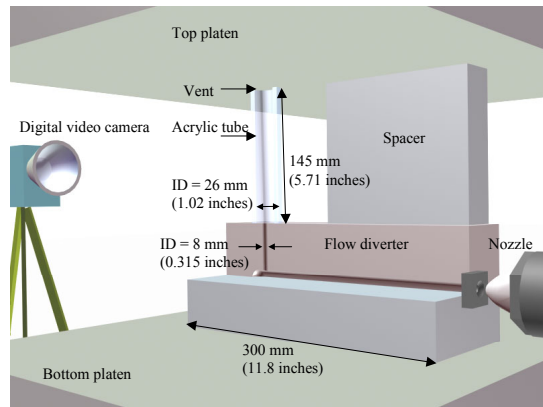


Figure 2: Schematic of the critical ingate velocity experiment.

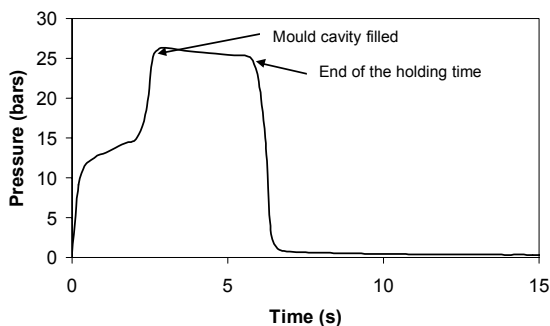


Figure 3: Injection pressure curve recorded

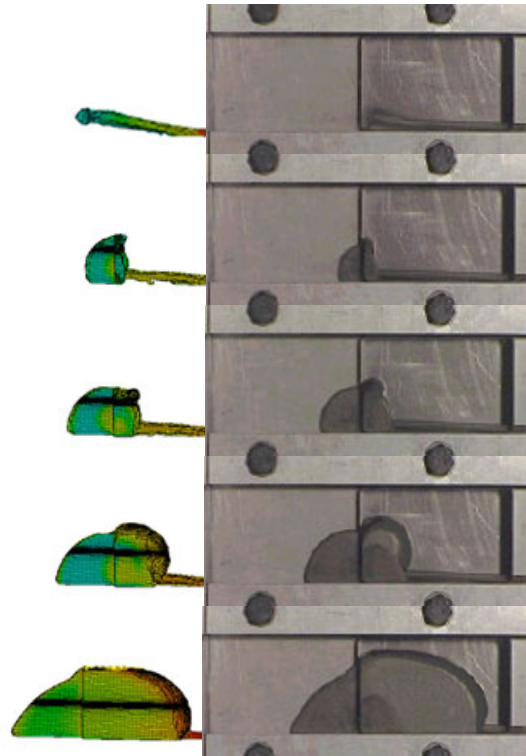


Figure 4: Comparison of the filling front predicted with Flow-3D® and that recorded experimentally at $t=0.08s$, $t=0.12s$, $t=0.20s$, $t=0.40s$ and $t=1.04s$

Fig.4 presents the simulation results, compared with the experimental results, during an injection from the second ingate position, at a temperature of 70°C, corresponding to a fully liquid wax, and a nominal injection pressure of 2.5 MPa (25 bars).

- At 0.08s, the wax starts to fill the cavity. It appears that the wax jumps into the cavity, due to the fact that the runner before the ingate is not horizontal and this creates a deflection. Both the simulation and the experiment show this phenomenon.
- At 0.12s, the wax enters the thin section as the jet hit its entrance. As the jet is larger than the thin section part of the wax stays in the thick section and the jet creates a recirculation phenomenon leading to the formation of a protuberance on the top of the wax.
- At 0.20s, the protuberance starts to move away from the thin section
- At 0.40s, less and less wax is going in the thin section, accelerating the filling of the thin section
- At 1.04s, the thick cavity is 60 to 80% filled whereas the thin cavity is only 20 to 30% filled.

All along, the simulation and the experiment have shown good agreement, with similar details appearing simultaneously in both of them. The model in the liquid state seems therefore to show a good predictability.

Paste state injection

Using the experimental apparatus shown in Fig.2, the influence of the gate velocity on the filling, and on the entrapment of air has been studied both in liquid and paste state. These experimental results have been used to

validate our model in the paste state. The simulations have been carried out using Flow-3D®.

Fig.5 presents results obtained during the injection of the wax in the liquid state, with a flow rate of $50 \times 10^{-6} \text{ m}^3 \cdot \text{s}^{-1}$ ($50 \text{ cm}^3 \cdot \text{s}^{-1}$), which corresponds to a gate velocity of $1 \text{ m} \cdot \text{s}^{-1}$. The comparison of simulation and experimental results, with the possible entrapment of air due to the initial jet, shows once more the prediction capability of our model in the liquid state.

Fig.6 presents the results obtained in the same gate velocity condition, but in the paste state. Here as well, the predictions of the model are in good agreement with experiments. An initial *worm* is created that enters the transparent tube and travels up it. In the simulation the *worm* touches the wall of the transparent tube and sticks to it giving a slightly different filling. Gravity then stops the progression of the *worm* in the tube and it starts to form a spiral until all the space below the *worm* is filled. As the wax continues to enter the cavity it pushes the wax already present in the tube and the *worm* is engulfed and disappears to be replaced by a cylinder of wax that fills the transparent tube.

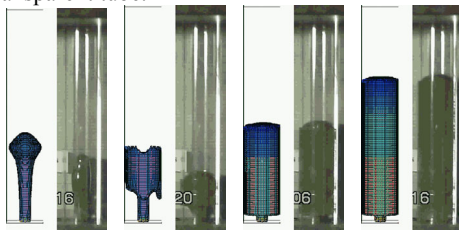


Figure 5: Comparison of experiments and simulation in the liquid state

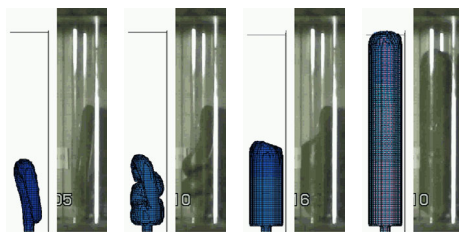


Figure 6: Comparison of experiments and simulation in the paste state

DEFECT PREDICTION

Predicting the appearance of defects is often a matter of interpretation of the results. Looking, for example, at the temperature of the *paste* as it flows in order to predict whether there will be a weld line when two flow fronts come together and the *paste* is cold. Some software companies have developed post-processing functions that are able to do this automatically thus reducing the post-processing time and the human interpretation. MoldFlow® has such capabilities for predicting weld-line defects together with other kind of defects such as air entrapment. Nevertheless, one limitation of MoldFlow® is its inability to predict jetting and therefore to deal with problem such as the two we have presented previously. The origin of this problem is the use of the Finite Element Method combined with a tetrahedral mesh that lead to a kind of so-called mesh diffusion which spreads the material in all directions instead of creating a stable jet.

However, for geometries where there is no jetting and where, in fact, you don't go from a thin to a very large

cross section the results given by MoldFlow® have proven to be good. So in this section, we will be using MoldFlow® to predict the appearance of weld-line defects using a suitable geometry shown in Fig.7. The die to make this part has been designed with 3 possible injection locations: one in the bottom of the cylinder (I_1) and two in the lateral face, in the thin wall section (I_2) and the medium wall section (I_3).

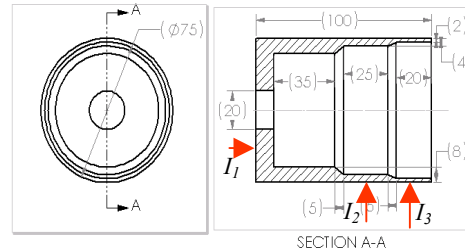


Figure 7: Cad drawing of the stepped wax pattern

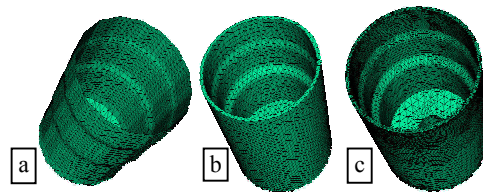


Figure 8: Different geometrical model available

Using MoldFlow® to carry out the simulation of the filling of the stepped cylinder, different geometrical models can be used. In MoldFlow®, three different approaches are available. Using a *midplane* mesh (Fig.8a) the 3D geometry is modelled by a simple plane which is meshed and each element is allocated a thickness. Using a *fusion* mesh (Fig.8b) the envelope of the surface is meshed and a finite difference method is used to calculate the velocity and thermal field throughout the thickness. Finally, using a *3D* mesh (Fig.8c) the whole volume is discretised. The use of one approach rather than another will obviously have an effect on the calculation time, the *midplane* approach being the fastest and the *3D* the slowest. The accuracy of the results may also be different with the different approaches. Table 1 shows a comparison of calculation time using the different models presented in Fig.9 running MoldFlow® (MPI 3.1) on a Dell WorkStation 530 with 2 Intel® Xeon™ 1.5GHz processors.

Mesh type	Number of nodes	Number of elements	Calculation time(s)
Midplane	1425	2780	231
Fusion	3408	6816	810
3D fast algorithm	16195	83568	2351
3D full Navier Stokes	16195	83568	16077

Table 1: Comparison of cpu time for different types of mesh

Presence of defect

Simulations and experiments have been carried out with the different injection locations, and different injection

flow rates. The simulations have been done with the three approaches.

Fig.9 shows results from simulation using the injection point I_3 . Results from the three types of mesh are shown.

Fig.10 presents pictures of parts injected using the three different injection point. Fig.10a corresponds to the simulation presented in Fig.9. It can be seen that the weld-line appears to correspond with the position where the filling front has stopped during the filling. Looking at the solidification *midplane* results, it appears that the stagnant part is nearly fully solid when the filling of the die finished. A post-processing function exists in MoldFlow® that can just outline the position of the welding line, as shown in Fig.11b for the second injection point.

Fig.11 presents the simulation results obtained with the second injection point I_2 . *Midplane* and *fusion* results are identical, so fusion results are not presented here. The 3D results give a miss-run prediction, in the thin section just above the injection point, whereas *midplane* and *fusion* predict a complete filling with a welding line as shown on Fig.11b. Comparison with the experiment, Fig.10b, shows that there are no mis-runs but there is a weld-line at the position predicted by the models. Here it can be noted that the weld-line is always predicted on the border of the elements, so the refinement of the mesh will have an impact on the geometry/position of the predicted position of the weld line. The mesh coarseness may therefore have an influence on the predicted position.

Fig.12 presents the results obtained with the injection point I_1 . Only the *fusion* results are shown as all the results were similar. For this injection point, little or no weld-

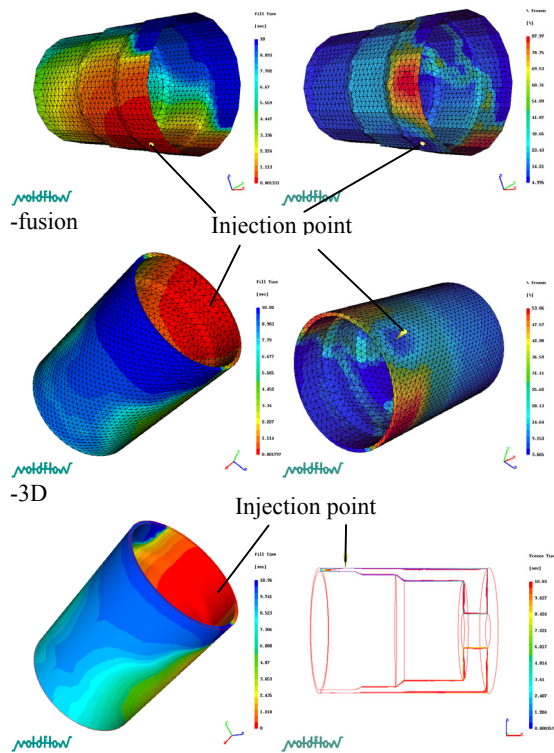


Figure 9: Filling time and solidified material for injection point I_3 with the 3 type of mesh. First column: Filling time/profile. Second column: %frozen/ freezing time

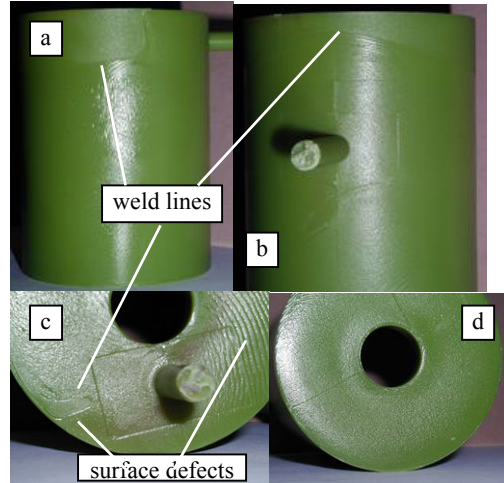


Figure 10: injected parts using the third injection point (a), the second injection point (b and d) and the first injection point (a)

lines are predicted. In fact only the fusion mesh predicted two weld lines, one in the inner corner and one on the flat face of the cylinder. No weld lines were found in the corner on the injected part. A small defect was apparent due to splashing at the beginning of the injection but it is not believe to correspond to the one predicted by the fusion model. Another type of defect was visible on this face as shown on the right of Fig.9c. This rippled surface is believed to be due to a too low velocity of the filling front together with a low surface temperature. This kind of defect is not apparent when using the injection point I_2 , as shown on Fig.9d.

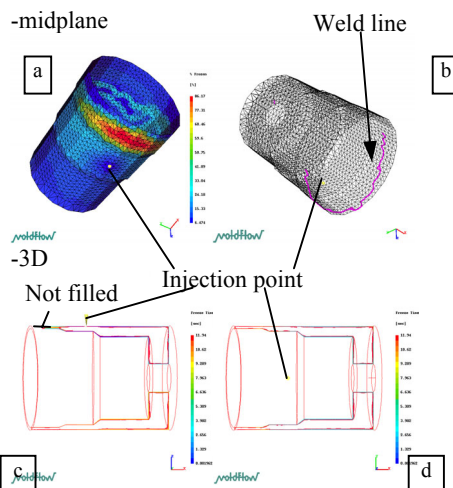


Figure 11: Simulation results with the second injection point (I_2), for *midplane* and 3D meshes

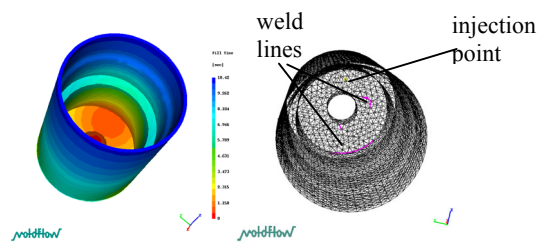


Figure 12: Results for the injection point (I_1) with fusion mesh

Position of defect

The prediction of occurrence of defect has proven to be accurate but the results presented up to now have not shown if the model was able to predict the right location of the defect. In the following only the injection point I_3 has been used. A range of flow rates has been used in order to change the position of the weld line. Only *midplane* and *fusion* meshes have been assessed. Experimentally it is not the weld line that has been looked for but the last position to fill in the die by making *short shots*.

Fig.13 presents the experimental results showing the angle between the injection point and the last section to fill. Top and bottom results are indicated, as the part is injected with the plane containing the axis of the cylinder and the injection point horizontal, so due to the effect of gravity two different angles can be measured.

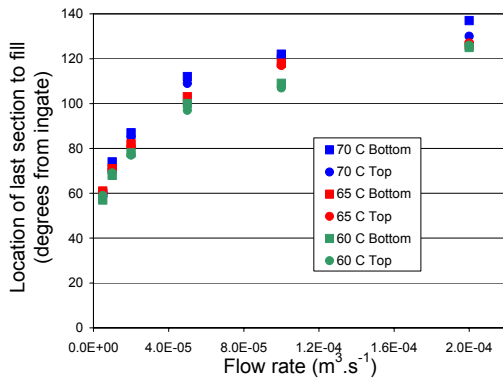


Figure 13: Position of the last section to fill determined experimentally

Fig.14 shows the measurement of the simulation results for one flow rate. The simulation has been carried out only at 70°C.

Fig.15 plots a graph of the experimental angle versus the predicted angle. If the predictions of the simulation were perfect the slope of this curve should be 1. It appears that the predictions using the *midplane* mesh give a slope of 1.03, which is reasonably good, whereas the predictions using the *fusion* mesh give a slope of 1.31, which is not as good. It was expected that the *fusion* mesh would have given better predictions than the *midplane* mesh as the geometrical definition of the component and the flow descriptions were more accurate. In the midplane model the flow is described by the mean velocity in the section whereas in the fusion model the velocity is described using an FD method. These results were submitted to MoldFlow® and their response was that the mesh was probably not good enough as the fusion mesh requires a good match of the elements on opposite faces of a volume, in order to make the finite difference scheme more accurate when computing the velocity and thermal fields.

CONCLUSION

This study has shown that it is possible to model accurately the filling of a die during the wax injection process, in both liquid and paste state. It has also shown that it is possible in some case to predict the formation of surface defects and to have a good estimation of their locations.

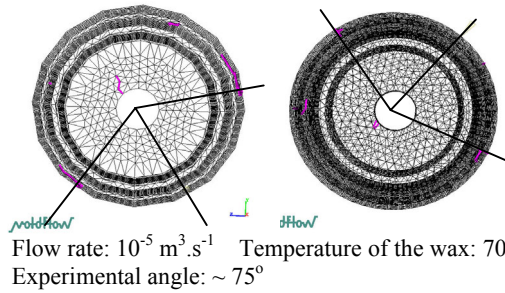


Figure 14: Measurement of the angle between the weld line and the injection point

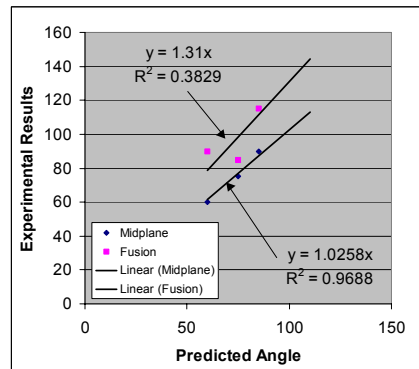


Figure 15: Correlation between predicted and simulated weld line positions

The different models used have been presented. It has been observed that the compressibility of the wax during the injection may not be significant due to the relatively low pressure involved in the case of mould filling. The Carreau model that has been used in Flow-3D® is complex, with a strong dependency of the viscosity on temperature and shear rate. This complex model involved large computation times. Therefore, from an industrial point of view it is interesting to look at possible simplifications to this model. The temperature variations during injection are not large, due to the low thermal diffusivity of the wax. So, as the injection process is a fast process, it may be possible to only calculate the temperature dependent terms at the beginning of the simulation and then only take into account the shear rate dependency.

ACKNOWLEDGEMENT

The authors want to acknowledge the financial support of EPSRC through the grant number GR/M60101 and the FOCAST project consortium. The co-worker of the authors, Jesus Cirre-Torres is also acknowledge for the extensive experimental work that he has done which has allowed this numerical work to be carried out.

REFERENCES

- S. CHAKRAVORTY, (1999), "Assessment of Properties of Investment Casting Waxes", *Proc. of 24th BICTA Conference on Investment Casting*, Oxford, UK, 6-8 June 1999,
- W. SIGFRIED and B. WADENIUS, "Study explores expansion/shrinkage behaviour of pattern waxes", *INCAST*, Vol. 13, n° 2, March 2000, pp14-16.